ACCSCIENCE PUBLISHING

Asian Journal of Water, Environment and Pollution

ORIGINAL RESEARCH ARTICLE

Experimental study on pollutant distribution around permeable spur dikes for river ecological engineering

Junhui He[1], Tao Yu[2]*, Dejian Wei[1], and Linfeng Han[2]

[1]Department of Engineering Management, Pinglu Canal Group Co., Ltd, Nanning, Guangxi, China

[2]National Engineering Research Center for Inland Waterway Regulation, Chongqing Jiaotong University, Chongqing, China

Abstract

Spur dikes play an important role in improving river ecology, and in engineering practice, permeable spur dikes with both stability and permeability are widely adopted. Based on generalized flume-model experiments, this study examines the distribution characteristics and mechanisms of insoluble pollutants around permeable spur dikes under different porosity and pore size conditions. The results indicate that high porosity or large pore size enhances water infiltration and jet effects, allowing more pollutants to enter and remain in downstream areas and recirculation zones; porosity and pore size have relatively little influence on pollutant concentration at the upstream slope but exert a greater impact on the recirculation zone and downstream slope; variations in flow discharge primarily regulate pollutant distribution by altering flow velocity and residence time. These findings suggest that by optimizing porosity and pore size, downstream pollutant accumulation can be reduced while maintaining structural stability, thereby balancing hydrodynamic exchange and habitat quality and providing important guidance for the design of ecological spur dikes.

Keywords: Permeable spur dike; Porosity; Pore size; Pollutant concentration

***Corresponding author:**
Tao Yu (yutao@cqjtu.edu.cn)

Citation: He J, Yu T, Wei D, Han L. Experimental study on pollutant distribution around permeable spur dikes for river ecological engineering. *Asian J Water Environ Pollut*. 2026;23(3):026050022. doi: 10.36922/AJWEP026050022

Received: January 28, 2026

Revised: March 7, 2026

Accepted: March 9, 2026

Published online: April 22, 2026

1. Introduction

The installation of spur dikes in river channels alters the original flow and sediment transport patterns.[1] Patel *et al.*[2] and Patel and Kumar[3] summarized that changes in the geometric parameters of spur dikes significantly affect the flow characteristics around them and studied how seepage through spur dikes influences substantial changes in riverbed elevation and scour depth. Jafari and Sui[4] emphasized the effect of spur dike azimuth on the size of scour holes, as well as the impact of ice cover on turbulence intensity. Qi *et al.*[5] proposed the use of U-shaped collars to reduce local scour around spur dikes and found that the collar's width, porosity, and length have pronounced effects on reducing scour, with permeable collars markedly lowering flow velocity and shear stress. Ding *et al.*[6] investigated how spur dike length and orientation influence flow patterns and turbulence characteristics in mildly curved channels.

While spur dikes regulate the transport of water and sediment, they also substantially

affect riverine ecological environments. Yang [7] suggested that spur dikes can affect habitat quality in the river reach by altering flow fields, velocity, water depth, and riverbed erosion–deposition patterns. Chung *et al.*[8] observed that the presence of spur dikes increases the formation of shallow pools and the abundance of fish and invertebrates. Huang *et al.*[9] found that the fish aggregation effect strengthens as flow diversity increases, with permeable spur dikes outperforming rubble-mound spur dikes in attracting fish. Li and Tong[10] summarized that channel-regulation structures can influence the physicochemical properties of river water, the structure and distribution of benthic communities, and fish habitats to varying degrees. Montazeri *et al.*[11] studied pollutant transport patterns around impermeable spur dikes and found that they can effectively shorten pollutant mixing lengths. Wan *et al.*[12] reported that dissolved oxygen rises significantly, while turbidity and velocity decrease markedly downstream of spur dikes, which also have a greater impact on plankton diversity indices compared to groynes parallel to the bank.

Przyborowski *et al.*[13] pointed out that spur dike groups and vegetation can influence the transport and deposition of floating macro-plastic debris, with low flow velocity and vegetation presence potentially inducing plastic deposition. Zhang *et al.*[14] revealed an asymmetric dispersion transport mechanism in layered porous media. Divya *et al.*[15] investigated the effects of floodplain inundation and riparian vegetation on hydrodynamics and material transport near spur dikes, finding that inundation and vegetation reduce anomalous scalar transport and accelerate its decay. Zhang *et al.*[16] conducted numerical simulations of low-water ecological restoration projects in straight river channels, demonstrating that restoration structures can effectively regulate flow patterns and enhance habitat heterogeneity. Zhao *et al.*[17] surveyed fish habitats in the Wutong River under ecological restoration and found that restoration measures improved water depth and flow diversity, increasing habitat suitability for fish, particularly in shallow and recirculation zones. Wang[18] examined the spatial distribution of nutrients around environmental restoration groynes, showing that these structures influence nutrient accumulation and diffusion, thereby affecting plankton growth and water quality. Zhao *et al.*[19] evaluated different ecological reoxygenation modes in urban rivers and reported that interventions such as jet and mixed aeration significantly enhanced dissolved oxygen levels, improving conditions for aquatic organisms and mitigating eutrophication. Zhang *et al.*,[20] based on vortex structures generated by artificial dams, reported that low-speed vortex zones with non-uniform flow are conducive to aggregating fish populations. Chen[21] studied the relationship between pollutant concentration fields and hydraulic characteristics in river confluence zones and concluded that the pollutant mixing position shifts toward the confluence as the confluence angle and aspect ratio increase. Yang[22] and Yang[23] primarily simulated pollutant diffusion in rivers using Mike software and found that turbulence has a considerable impact on pollutant concentration attenuation.

The above studies show that spur dikes play multiple roles in regulating water–sediment movement and maintaining river ecological health. Modifications to flow structure, local velocity, turbulence characteristics, and riverbed morphology directly affect sediment erosion and deposition, as well as biological habitats.[24-27] Permeable spur dikes, in particular, can simultaneously meet flood control and channel regulation functions while providing a more heterogeneous flow environment and shelter to promote fish aggregation and aquatic biodiversity. Currently, multiple ecological conservation zones are being established in tributary confluence reaches of the Pinglu Canal under construction, where permeable spur dikes are needed to enhance the canal's ecological function. When tributary flows enter the canal, they may carry pollutants; pollutant diffusion in rivers follows distinctive patterns, yet most studies on the impacts of pollutant diffusion have not considered the role of hydraulic structures. Therefore, it is necessary to investigate the influence of spur dikes on pollutant diffusion. River pollutants are generally classified as soluble or insoluble. Our study specifically investigates the distributional impacts of spur dikes on point-source insoluble pollutants to establish patterns and examine how permeable characteristics of spur dikes influence pollutant concentration distributions in fluvial environments.

2. Methods

2.1. Experimental instruments and equipment

The experiment was conducted in a 30 m × 2 m × 1 m (length × width × height) rectangular glass flume. Inlet discharge was controlled by an automatic flow measurement and control system, co-developed by Tsinghua University and Beijing Shangshui InfoTech Co., Ltd. Water depth measured at the toe of the spur dike's upstream slope was regulated using a point gauge (i.e., a water level gauge).

The permeable spur dike model flume is shown in Figure 1. The main instruments and equipment used in the experiment are shown in Figure 2.

2.2. Pollutant simulation and measurement methods

The experiment used dyed quartz sand (median particle size $D_{50} \approx 0.1$ mm) as a surrogate material for insoluble pollutants. This material was selected because its particle-

Figure 1. Experimental model flume

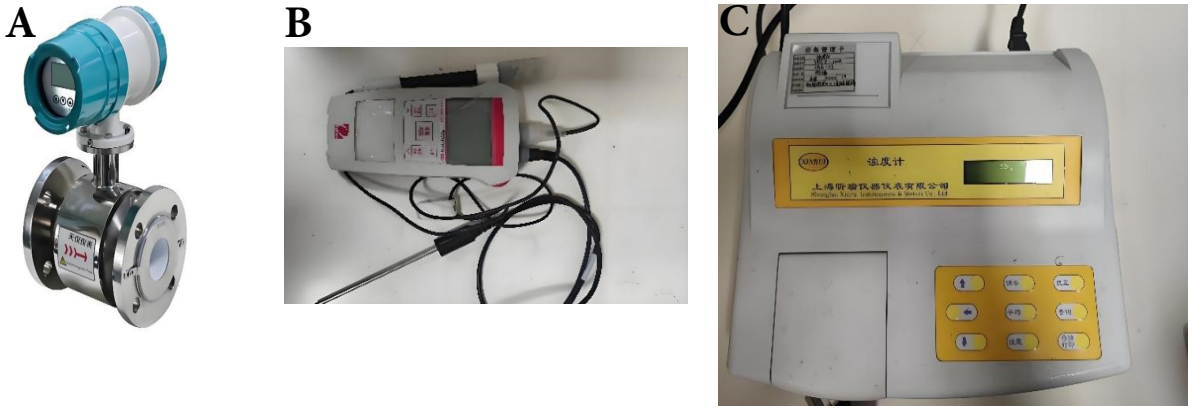

Figure 2. Experimental instruments. (A) Electromagnetic flowmeter. (B) Portable dissolved oxygen meter. (C) Photoelectric turbidity meter.

size range and density are similar to those of natural fine silt and certain organic particulates (e.g., detrital organic matter), and it exhibits comparable hydrodynamic behavior in suspension in river channels, with similar settling velocities and resuspension responses under the same flow conditions. Li *et al.*[28] showed a significant positive correlation between suspended sediment concentration and turbidity; therefore, turbidity (in Nephelometric turbidity unit [NTU]) was employed in this study as an indicator to quantify the concentration of suspended particles.

Turbidity was measured via a portable photoelectric turbidimeter (WGZ-200A, Nanbei Instrument Limited, China). The spatial arrangement of pollutant concentration monitoring points and cross-sections is illustrated in Figure 3.

2.3. Model design

2.3.1. Spur dike model design

Based on statistical analysis of spur dike dimensions in the upper reaches of the Yangtze River and the actual

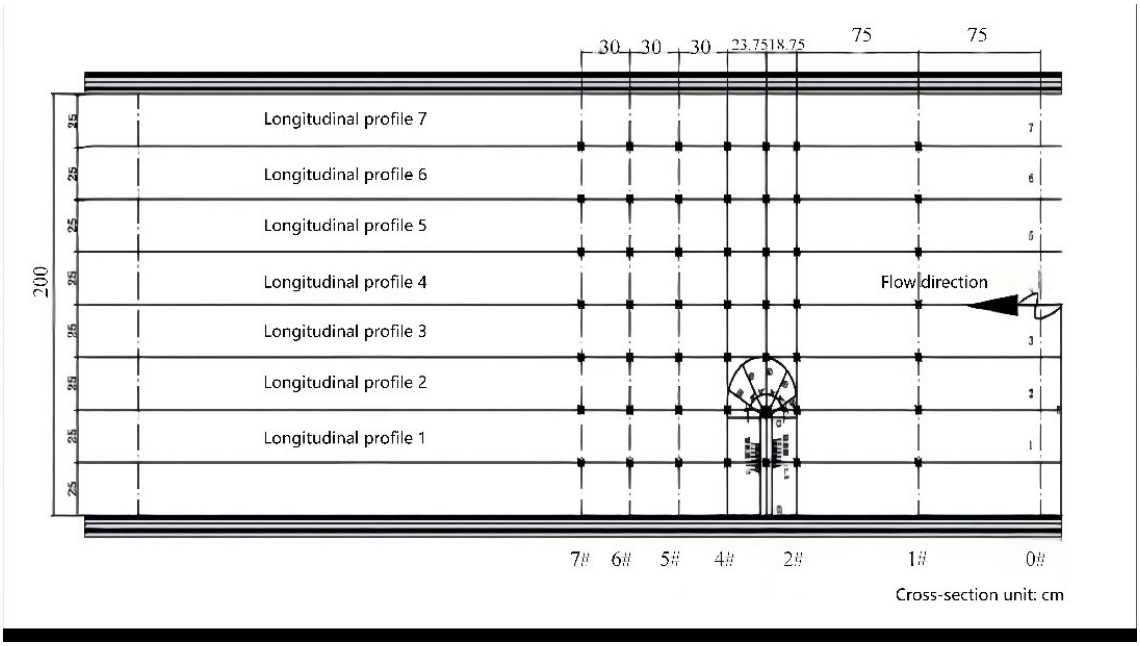

Figure 3. Layout of test pollutant concentration measurements

width of the experimental flume, the permeable spur dike parameters were determined as follows: length 50.0 cm, height 10.0 cm, crest width 7.5 cm, and base width 42.5 cm. The cross-section adopted a trapezoidal shape with an arc-shaped straight head; the upstream slope ratio was 1.0:1.5, and the downstream slope ratio was 1:2.0 (as shown in Figure 4).

In the experiment, the pores of the permeable spur dike were circular. Three pore diameters (R) were examined: 16 mm, 20 mm, and 32 mm. The spur dike angle in the model test was 90°. By combining different porosity levels (P1 = 6.8%, P2 = 14.1%, P3 = 22.5%), different pore sizes (R1 = 16 mm, R2 = 20 mm, R3 = 32 mm), 27 sets of test conditions were conducted. The test conditions are detailed in Table 1.

2.3.2. Flow data source and statistical analysis

The experimental flow values used in this study are based on daily flow measurements from the Luwu Hydrological Station along the Pinglu Canal, spanning 1959 to 2021 (63 years). The Luwu Hydrological Station is located in Luwu Town, Lingshan County, in the middle and upper reaches of the Qin River. It is a national basic hydrological station in China. Flow measurements were conducted in accordance with site conditions using the velocity–area and current–meter methods, following the standard procedures recommended by relevant hydrological guidelines, such as the Specifications for River Discharge Measurement (GB 50179-2015).[29] Instruments are calibrated regularly, and the data are checked for consistency and completeness. Suspicious or missing values are carefully evaluated and corrected according to hydrological standards. In addition, the cross-section at the Luwu Hydrological Station has stable channel geometry and well-defined banks (Figure 5), and is therefore selected as the typical control section for the experimental study reach.

To more accurately evaluate the hydraulic and pollutant transport patterns of spur dikes under the conditions of this river section, we conducted fundamental attribute analysis, overall statistical analysis, and seasonal statistical analysis on the measured flow data.

(i) Basic data information

Table 2 presents basic information on the flow data, including data length, time resolution, observed flow range, and proportion of missing values. There were 0% zero values. The station's flow data records show good continuity and the overall missing-data rate is less than 1%.

(ii) Overall and seasonal statistics

To comprehensively assess the data characteristics, annual statistics over 63 years and seasonal statistics of daily average flow from May to October each year were calculated. The results are shown in Table 3. The mean coefficient of variation of streamflow in the Pinglu Canal was approximately 2.1, consistent with Dimitriadis *et al.*'s[30] findings that the global mean coefficient of variation of streamflow, estimated from thousands of runoff stations, ranged from 1.7 to 2.4. This indicates that the streamflow

samples from the Luwu Hydrological Station are of high quality and capable of capturing the long-term variability of streamflow processes.

From Table 3, it can be seen that the mean flow during May–October is higher than the annual mean, and the variability is also greater, reflecting the substantial replenishment effect of the flood season and inflow from tributaries on the main channel flow.

Table 1. Experimental conditions

Pore size (R, mm)	Porosity (P, %)	Flow discharge (Q, [L·s^{-1}]); water depth (H, cm)
16	6.8	65; 11
		95; 14
		135; 17
	14.1	65; 11
		95; 14
		135; 17
	22.5	65; 11
		95; 14
		135; 17
20	6.8	65; 11
		95; 14
		135; 17
	14.1	65; 11
		95; 14
		135; 17
	22.5	65; 11
		95; 14
		135; 17
32	6.8	65; 11
		95; 14
		135; 17
	14.1	65; 11
		95; 14
		135; 17
	22.5	65; 11
		95; 14
		135; 17

Table 2. Primary attributes of the prototype streamflow dataset

Station name	Record length (years)	Time step	Range (m^3/s)	Missing values (%)
Luwu Hydrological Station	63 (1959–2021)	Daily	0.2–1190.0	0.06

Table 3. Marginal and seasonal statistics of prototype streamflow data

Statistical type	Multi-year average (m^3/s)	Standard deviation	Annual average maximum (m^3/s)	Annual average minimum (m^3/s)
Annual	38.7	111.6	240	0.2
May–October	89.4	128.5	852	8.2

(iii) Model scale and experimental conditions

According to investigations, tributaries along the Pinglu Canal are most likely to carry pollutants from May to October each year, and pollutants diffuse rapidly during major flood periods. Therefore, this paper primarily investigates the impact of spur dike permeability characteristics on pollutant diffusion during flood periods. This study statistically analyzed the measured flow data from May 1 to October 31 each year between 1959 and 2021 from Luwu Station. Combined with topographic data from the Luwu Station cross-section, it was calculated that the cross-sectional average velocity corresponding to the three largest flood events from May to October each year ranged from 2.0 to 2.5 m/s.

Considering the laboratory flume scale and equipment constraints, a generalized geometric scale of 1:40 was adopted. The corresponding depth scale and velocity scale were 1:40 and 1:6.325, respectively. The calculated model depth and velocity are shown in Table 4.

The experimental flume width was 2 m. Considering the relationship between flow rate and water depth, three representative model flow rates (65 L/s, 95 L/s, and 135 L/s) were selected for model testing, corresponding to

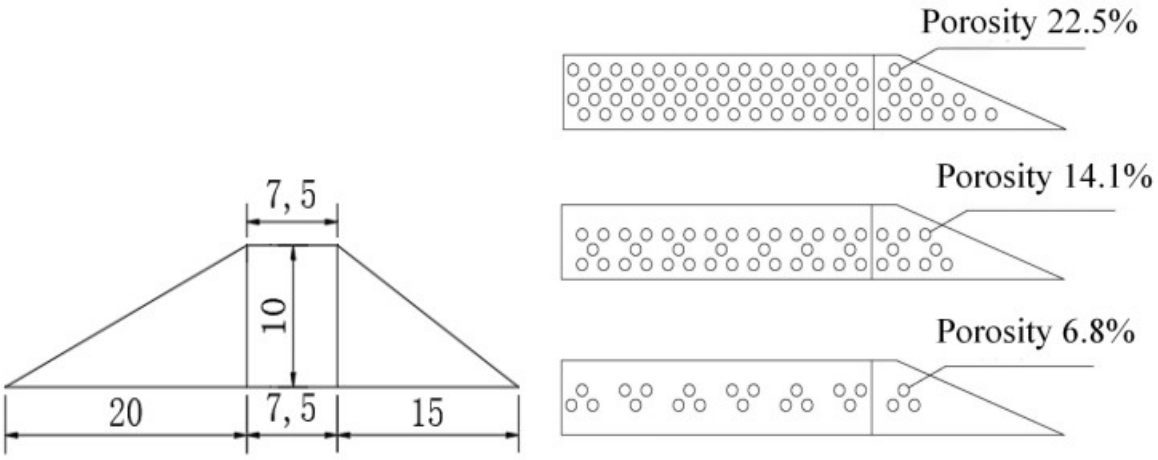

Figure 4. Cross-section and longitudinal section of a spur dike
Note: Length in cm.

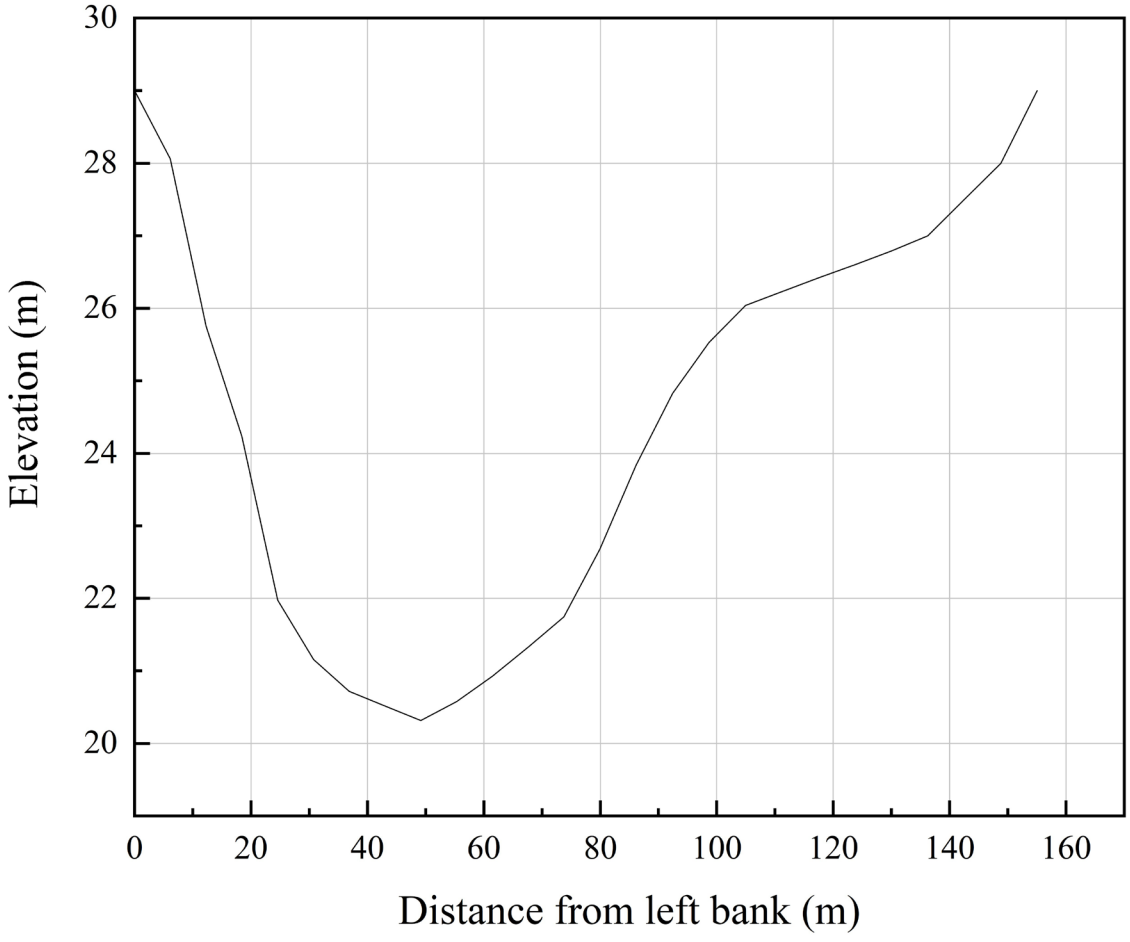

Figure 5. Cross-section at Luwu Hydrological Station

water depths of H = 11 cm, 14 cm, and 17 cm, respectively, as shown in Table 1.

Table 4. Prototype and model hydraulic parameters

Prototype hydraulic parameters	Model hydraulic parameters
Flood period flow (m^3/s): 411–1,190	Model flow (L/s): 65–135
Average depth (m): 4.4–6.8	Model depth (cm): 11–17
Channel flow area (m^2): 220–476	Model velocity (m/s): 0.3–0.4

3. Results and discussion

To investigate pollutant distribution patterns around the permeable spur dike, a comparative analysis was performed. Pollutant concentrations were examined at three locations: the upstream slope (Cross-section 2#), the downstream slope (Cross-section 4#), and the recirculation zone (Cross-section 5#). These concentrations were analyzed with respect to variations in flow discharge, porosity, and pore size.

3.1. Impact of flow discharge on pollutant concentrations around the spur dike

Under experimental conditions with a pore size of 20 mm and a porosity of 6.8%, the influence of different flow discharges (Q1 = 65 L/s, Q2 = 95 L/s, Q3 = 135 L/s) on pollutant concentration was analyzed. The analysis focused on the upstream slope (Cross-section 2#), the downstream slope (Cross-section 4#), and the recirculation zone behind the dike (Cross-section 5#). The results are shown in Figures 6–8.

3.1.1. Analysis of pollutant concentration variation at the upstream slope

Figure 6 shows that at Cross-section 2# (toe of the upstream slope), the largest lateral concentration gradient was observed within the length range of the spur dike, indicating that this area was the direct influence zone of the spur dike. Beyond 100 cm, concentration differences become minimal. Under identical pore size (R = 20 mm)

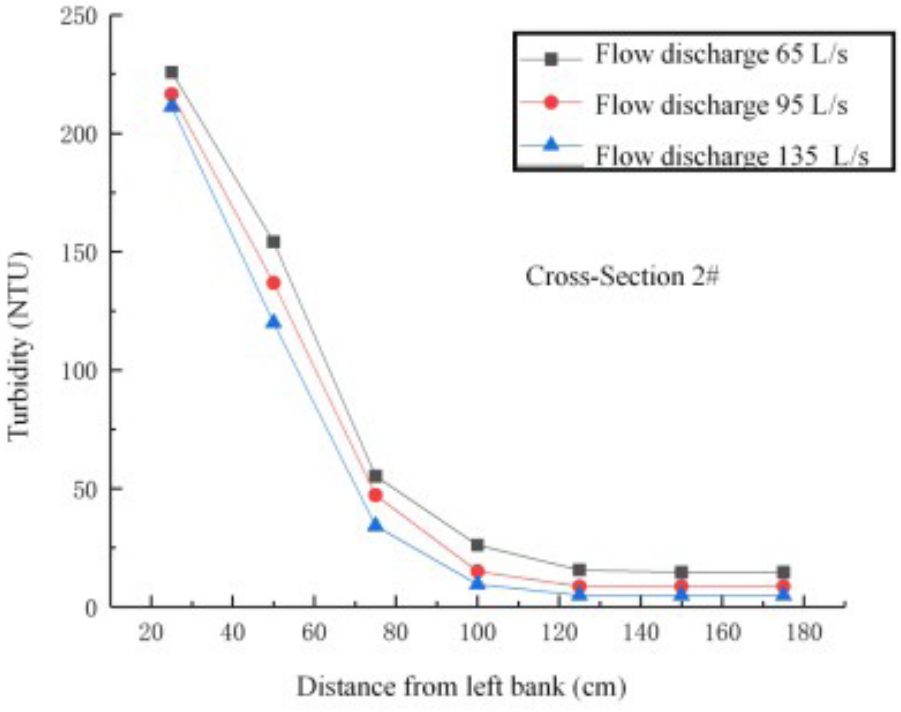

Figure 6. Concentration distribution of pollutants on the upstream slope (Cross-section 2#) under different flow conditions

and porosity (P = 6.8%) conditions, when the discharge increased from 65 L/s to 135 L/s, the mean concentration decreased by 15.4%, with the greatest drop occurring near the dike root. This indicates that the advection velocity of pollutant particles within the upstream influence zone increases, resulting in their rapid transport out of the zone.

According to findings from a previous study, for identical porosity (P) and pore size (R), the upstream flow velocity on the upstream slope increases markedly with increasing discharge, while the velocity distribution remains relatively uniform.[31] In our study, when Q = 65 L/s, the mean flow velocity was approximately 0.18 m/s; when Q = 135 L/s, it rose to about 0.26 m/s (an increase of around 44%), which accelerated the downstream dispersion of suspended particles, reduced their deposition in the near-shore zone of the upstream slope, and consequently led to a decline in pollutant concentration.

3.1.2. Analysis of pollutant concentration variation at the downstream slope

As shown in Figure 7, the overall variation of pollutant concentration on the downstream slope (Cross-section 4#) followed a decreasing trend from the left bank to the right bank. The concentration gradually stabilized at 125 cm from the left bank. Under identical pore size and porosity conditions, higher flow discharges led to greater pollutant concentrations on the downstream slope (Cross-section 4#). Compared to the upstream slope, pollutant concentrations here were remarkably lower. Additionally, the variation in concentration across different flow discharges was slightly greater than observed on the upstream slope.

According to a previous study, in the mainstream zone along the right bank of the downstream slope, the flow velocity increases with discharge under identical pore size and porosity conditions, accompanied by an enhancement in the energy of over-dike flow.[29] For instance, when Q = 65 L/s, the velocity near the dike head was approximately 0.22 m/s, whereas at Q = 135 L/s it reached about 0.31 m/s (an increase of around 41%). The high-velocity plunging flow over the dike intensified sediment resuspension and mixing in the downstream water body, while the area behind the dike formed a recirculation zone, together leading to an increase in downstream slope pollutant concentration with rising discharge.

3.1.3. Analysis of pollutant concentration variation in the recirculation zone

Figure 8 shows that the pollutant concentration in the recirculation zone behind the dike (Cross-section 5#)

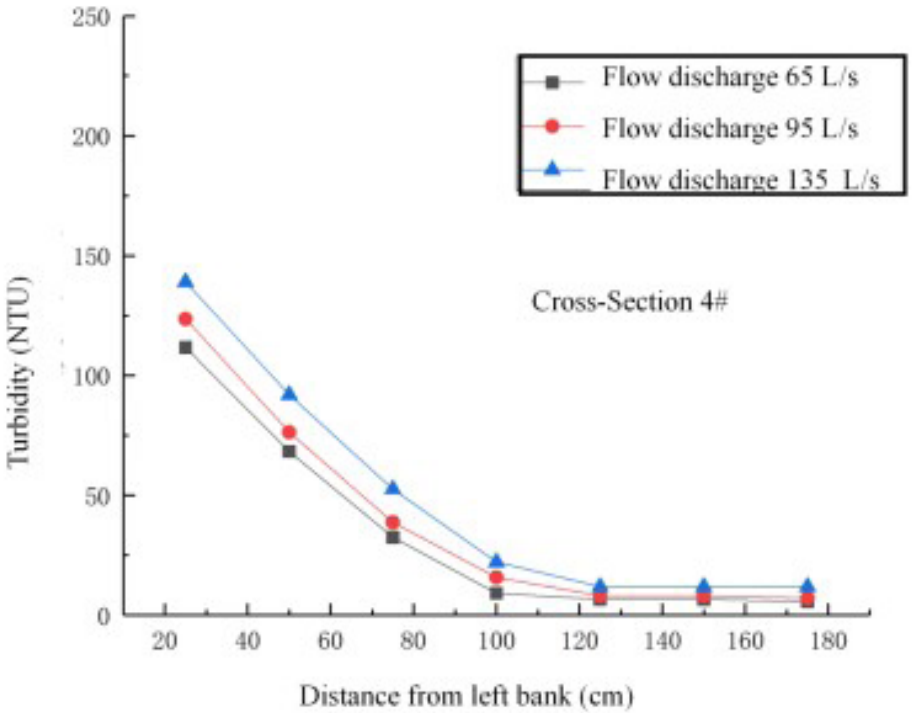

Figure 7. Concentration distribution of pollutants on the downstream slope (Cross-section 4#) under different flow conditions

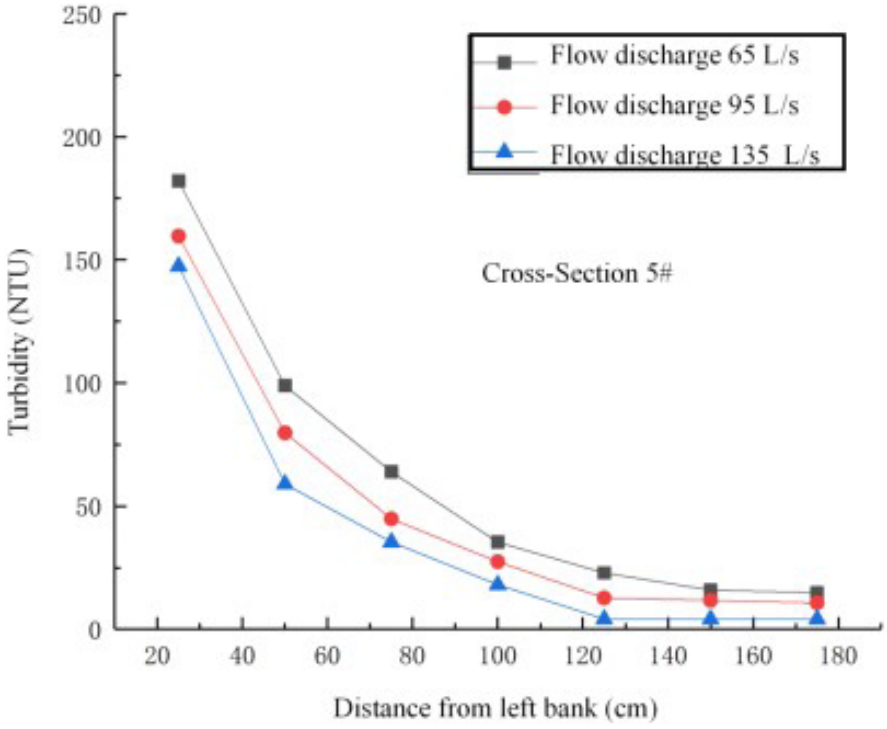

Figure 8. Pollutant concentration distribution in the recirculation zone behind the dike (Cross-section 5#) under different flow conditions

generally decreased from the left bank to the right bank and then gradually stabilized. Under conditions of identical porosity and pore size, higher flow discharges resulted in smaller pollutant concentrations in the recirculation zone. The concentration differences were substantially influenced by flow discharge. Compared to the downstream slope, pollutant concentrations increased here. Smaller flow discharges led to greater pollutant deposition and higher concentrations.

Based on Figures 6–8, when the discharge increased from 65 L/s to 135 L/s, the mean pollutant concentration on the upstream slope decreased by 15.4% (from 42.3 NTU to 35.8 NTU), that on the downstream slope increased by 8.4% (from 28.5 NTU to 30.9 NTU), and that in the recirculation zone behind the dike decreased by 12.1% (from 30.4 NTU to 26.7 NTU). Overall, the concentration in the recirculation zone was approximately 8–10% higher than that on the downstream slope, but about 15–18% lower than that on the upstream slope.

3.2. Impact of porosity on pollutant concentrations around the spur dike

Using a pore size of 16 mm, a flow discharge of 95 L/s, and three porosities (P_1 = 6.8%, P_2 = 14.1%, P_3 = 22.5%) as the test conditions, this study analyzed the influence of porosity on pollutant concentrations at three key locations. These locations included the upstream slope (Cross-section 2#), the downstream slope (Cross-section 4#), and the recirculation zone downstream of the spur dike (Cross-section 5#). The results are presented in Figures 9–11.

3.2.1. Analysis of pollutant concentration variation at the upstream slope

For different porosity levels (6.8–22.5%), at Cross-section 2#, the most pronounced concentration decrease occurred within the spur dike length range. This is because fluid velocity increases as it passes through the pores, thereby reducing the number of pollutant particles. Beyond 100 cm from the left bank, concentrations tend to stabilize, indicating that the influence range of the spur dike is limited. Higher porosity reduced the mean upstream slope concentration by up to 14.5%, but it also increased local variability near the structure, as enhanced through-flow produced a larger turbulence zone in this area compared to sections without the spur dike (Figure 9).

3.2.2. Analysis of pollutant concentration variation at the downstream slope

As shown in Figure 10, the overall variation in pollutant

concentration on the downstream slope (Cross-section 4#) followed a distinct pattern: it gradually decreased from the left bank to the right bank, eventually stabilized, and the magnitude of variation diminished. Across different porosities, this concentration variation was substantial: the pollutant concentration was higher near the left bank and stabilized at 125 cm from the left bank. Notably, higher porosity corresponded to higher pollutant concentration on the downstream slope. Compared to the upstream slope, the pollutant concentration on the downstream slope was substantially lower, and its changes were slower.

3.2.3. Analysis of pollutant concentration variation in the recirculation zone

Figure 11 shows pollutant concentrations in the recirculation zone (Cross-section 5#). Concentrations decreased gradually from the left bank to the right bank. They stabilized at 125 cm from the left bank. Different porosity levels caused slight variations in concentration. Higher porosity increased concentrations in the recirculation zone. Concentrations showed no notable difference from those at the downstream slope. Higher porosity increased pollutant deposition, resulting in higher concentrations in the recirculation zone. This is because in the recirculation zone, an increase in porosity allows more mainstream flow to enter the vortex region;[29] when P = 22.5%, the inflow velocity at the left-bank entrance increased by approximately 0.04 m/s, thereby raising the local flow velocity and transporting more particles into this area.

Based on the data in Figures 9–11, when the porosity increased from 6.8% to 22.5%, the mean pollutant concentration on the upstream slope decreased by 14.5% (from 39.8 NTU to 34.0 NTU), that on the downstream slope decreased by 16.7% (from 27.6 NTU to 23.0 NTU), and that in the recirculation zone increased by 9.8% (from 26.8 NTU to 29.4 NTU). Under the same conditions, the downstream slope concentration was, on average, about 16% lower than before passing through the spur dike, and the difference between the recirculation zone and downstream slope concentrations was small.

3.3. Impact of pore size on pollutant concentrations around the spur dike

Using a porosity of 22.5%, a flow discharge of 135 L/s, and three different pore sizes (R1 = 16 mm, R2 = 20 mm, R3 = 32 mm) as the test conditions, we analyzed the influence of pore sizes on pollutant concentrations at the upstream slope (Cross-section 2#), downstream slope (Cross-section 4#), and recirculation zone downstream of the spur dike (Cross-section 5#). The results are presented in Figures 12–14.

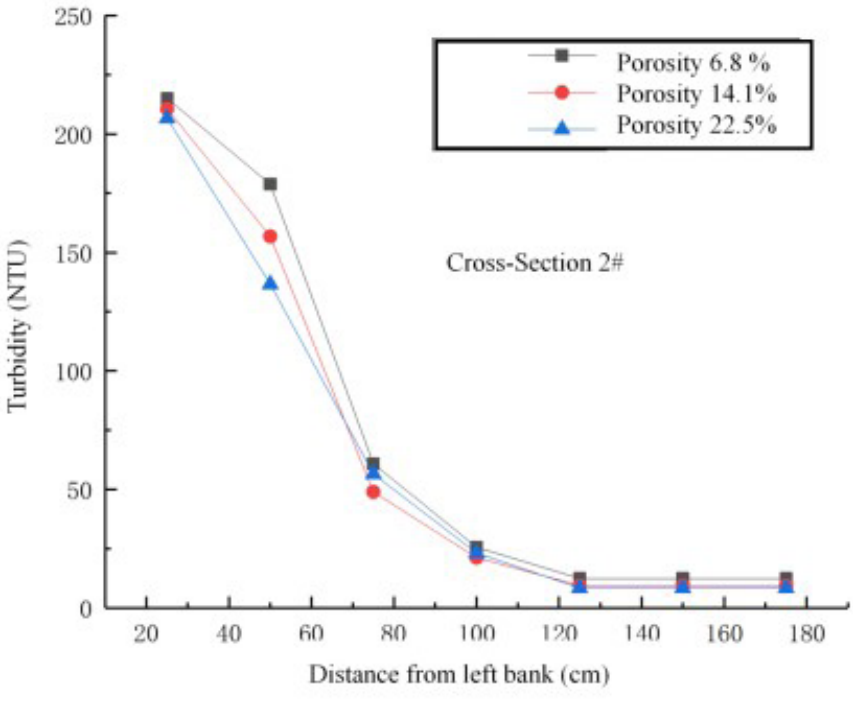

Figure 9. Concentration distribution of pollutants on the upstream slope (Cross-section 2#) under different porosities

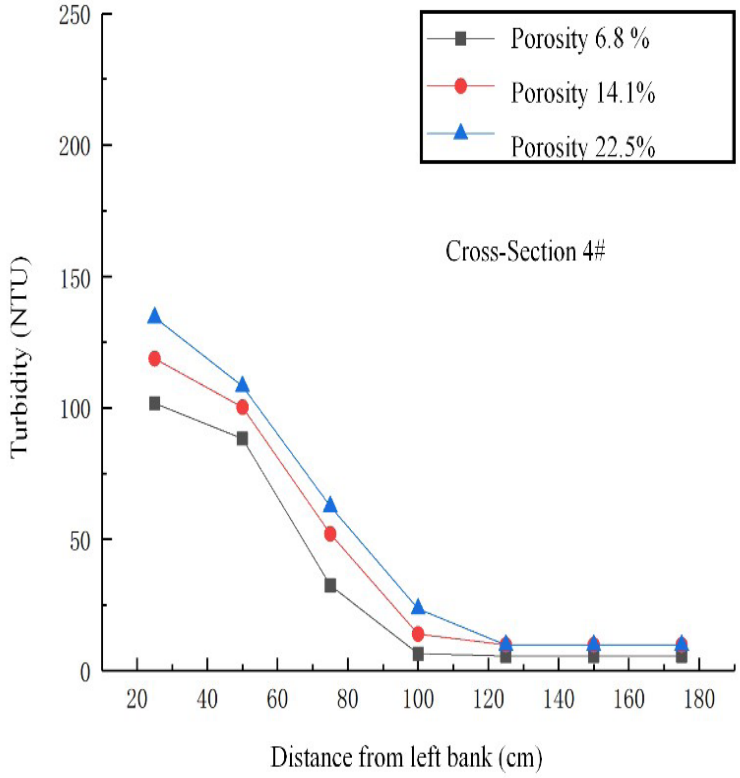

Figure 10. Concentration distribution of pollutants on the downstream slope (Cross-section 4#) under different porosity conditions

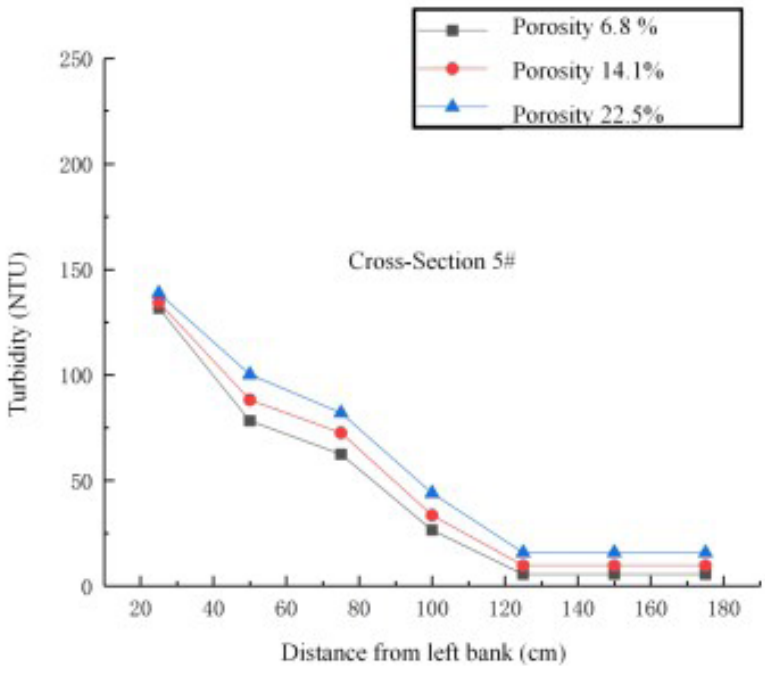

Figure 11. Concentration distribution of pollutants in the recirculation zone behind the dike (Cross-section 5#) under different porosity conditions

3.3.1. Analysis of pollutant concentration variation at the upstream slope

From Figure 12, it is evident that the concentration distribution curve at Cross-section 2# shows a pronounced lateral gradient within the spur dike length range, reflecting localized disturbances due to pore jets. The concentration remained essentially constant beyond approximately 125 cm, indicating that the mainstream flow field dominated. Larger pore sizes resulted in lower pollutant concentrations at the upstream slope toe, further confirming that changes in permeability can create different pollutant transport pathways, and that high flow velocity limits the ability of pore size to influence particle retention within the upstream influence zone.

3.3.2. Analysis of pollutant concentration variation at the downstream slope

Figure 13 shows pollutant concentrations at the downstream slope (Cross-section 4#). Concentrations decreased gradually from the left bank to the right bank. They stabilized at 100 cm from the left bank. Different pore sizes led to notable variations in pollutant concentrations. The flow velocity in the mainstream zone along the right bank of the downstream slope increased substantially with pore size (approximately 0.24 m/s for R = 16 mm and 0.29 m/s for R = 32 mm),[29] enhancing particle resuspension and lateral transport, thereby leading to lower pollutant concentrations. Therefore, under constant flow discharge, larger pore sizes decrease pollutant concentrations on the downstream slope. Concentrations were higher than those at the upstream slope. Smaller pore sizes produced smaller concentration variations.

3.3.3. Analysis of pollutant concentration variation in the recirculation zone

Figure 14 shows pollutant concentrations in the recirculation zone (Cross-section 5#). Concentrations decreased gradually from the left bank to the right bank. They stabilized at 125 cm from the left bank. Different pore sizes resulted in notable variations in pollutant concentration. Under constant flow discharge, larger pore sizes increased pollutant concentrations in the recirculation zone. Concentrations in the recirculation zone exceed those at the downstream slope due to the spur dike effects. Larger pore sizes increased pollutant deposition, thus increasing turbidity.

Based on Figures 12–14, when the pore size increased from 16 mm to 32 mm, the mean pollutant concentration on the upstream slope decreased by approximately 6.3% (from 37.5 NTU to 35.2 NTU), that on the downstream slope increased by 11.5% (from 26.0 NTU to 29.0 NTU), and that in the recirculation zone increased by 13.2%

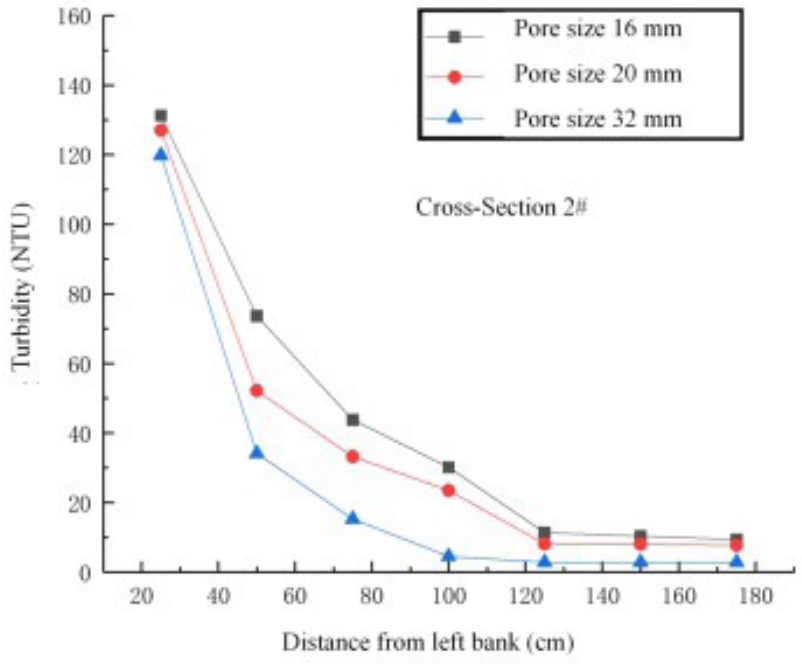

Figure 12. Concentration distribution of pollutants on the upstream slope (Cross-section 2#) under different pore sizes

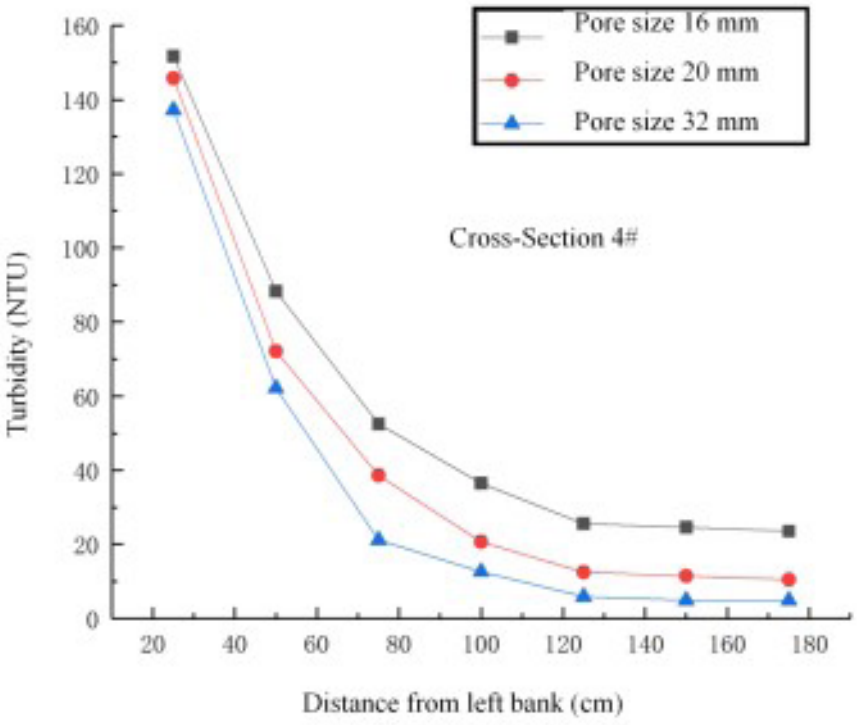

Figure 13. Pollutant concentration distribution on the downstream slope (Cross-section 4#) under different pore sizes

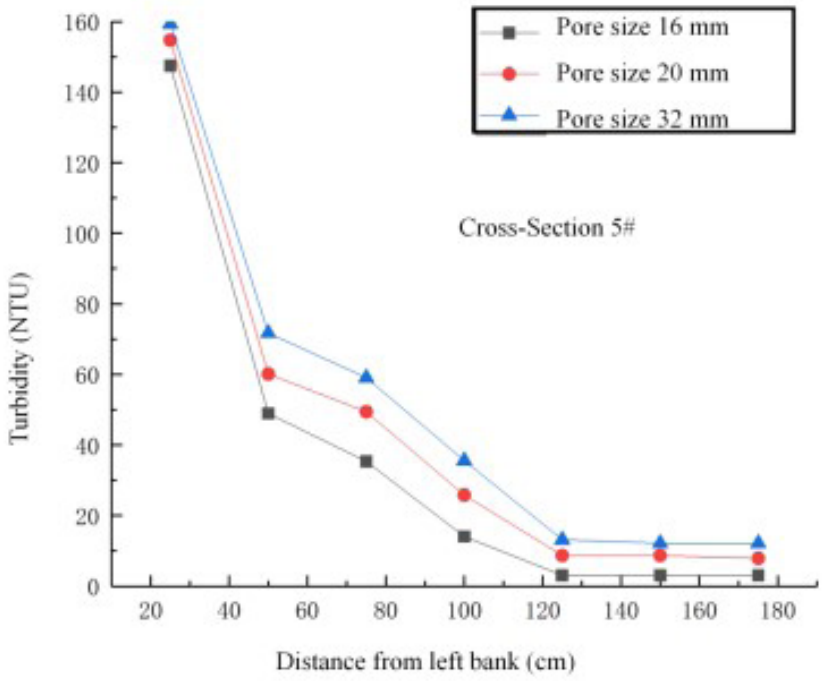

Figure 14. Pollutant concentration distribution in the recirculation zone behind the dike (Cross-section 5#) under different pore sizes

(from 28.1 NTU to 31.8 NTU). Overall, pore size had a more substantial influence on pollutant concentrations on the downstream slope and in the recirculation zone, while its effect on the upstream slope was comparatively minor.

3.4. Limitations

This study employed generalized flume model experiments under clear-water and fixed-bed conditions to simulate the transport and distribution patterns of insoluble pollutants around permeable spur dikes under varying flow discharge (Q), porosity (P), and pore size (R). It should be noted that the experiments have the following limitations: (i) Simplified inflow and sediment conditions. The experiments were conducted under clear-water, steady-flow conditions, excluding sediment-laden flows, mixed-pollutant scenarios, or unsteady flow conditions. Therefore, they cannot reflect the effects of flow nonstationarity, sediment–pollutant coupling, or flocculation processes. (ii) Simplified bed morphology. The fixed-bed setup cannot simulate the scour and deposition dynamics of the riverbed near the spur dike, neglecting interactions between bedform changes and pollutant resuspension. (iii) Single-mode pollutant release. Pollutants were introduced via point-source releases, without accounting for areal sources or multiple-source diffusion scenarios, thus failing to fully represent pollutant input characteristics in natural rivers.

These limitations imply that the research findings are mainly applicable for explaining the instantaneous spatial distribution patterns of particulate pollutants under controlled hydrodynamic conditions. When applying them to real-world river engineering, corrections and validation should be conducted using long-term prototype hydrological records and more complex field conditions.

The limitations of our approach include: (i) dyed quartz sand does not possess the biochemical properties of real organic particles and thus cannot reflect flocculation or biodegradation processes; (ii) the density and shape of quartz sand differ slightly from those of natural materials, which may affect the critical incipient velocity and settling process. Given that the results of this study primarily reflect the patterns of particulate pollutant spatial distribution driven by hydrodynamic conditions—without examining particle changes driven by biological or chemical processes—and that the quartz sand used has a relatively small particle size, the interpretation of results is limited to hydrodynamic influences on particulate pollutant distribution. Therefore, this experimental approach is considered appropriate.

3.5. Significance for ecological spur dike design

The experimental results show that the porosity and pore size of permeable spur dikes markedly regulate pollutant concentrations on the downstream slope and in the recirculation zone behind the dike, while the impact on the upstream slope is relatively weak. The following recommendations can be considered in ecological spur dike design:

(i) Higher porosity and larger pore size enhance the permeability of the dike and the over-dike jet effect, leading to more pollutants flowing into the downstream slope and recirculation zone. However, the downstream slope is subject to dual effects of seepage flow under the dike and free surface flow, making it difficult for pollutants to accumulate there. In contrast, the downstream recirculation zone has a lower flow velocity, and pollutants are easily captured by low-velocity vortices, thereby increasing the risk of pollutant accumulation in the recirculation zone.
(ii) Lower porosity and smaller pore size weaken the permeable channel effect, reducing pollutant entry into the downstream slope and recirculation zone, which helps protect downstream fish habitats and water quality, but may lead to increased deposition on the upstream slope and localized pollutant enrichment.
(iii) Flow regulation can serve as a supplementary measure: by lowering peak flows during specific seasons or ecologically sensitive periods, the transport and accumulation of pollutants in the recirculation zone can be reduced.

Therefore, in ecological navigation channel and river restoration projects, designers can select appropriate combinations of porosity and pore size based on the target habitat type and pollution control needs, in conjunction with riverbed morphology and upstream flow characteristics, to balance structural stability, hydrodynamic exchange, and habitat quality. For example, to reduce pollutant accumulation in downstream fish habitats (located in the recirculation zone), a spur dike configuration with 15% porosity and a pore size of 0.5 m can be adopted. If the goal is to promote water exchange and material cycling in the reach, porosity and pore size can be increased moderately, but attention must be paid to the stability of the structure itself.

4. Conclusion

A flume generalized model was used. It investigated key

factors affecting pollutant transport near spur dikes. These factors included flow discharges, porosity, and pore size. The key findings are as follows:

(i) When pore size and porosity are identical, pollutant concentration on the upstream slope of the spur dike and in the recirculation zone behind the dike is negatively correlated with flow discharge, while pollutant concentration on the downstream slope is positively correlated with flow discharge. Overall, concentrations in the recirculation zone are about 8–10% higher than those on the downstream slope, and about 15–18% lower than those on the upstream slope.

(ii) When flow discharge and pore size are identical, pollutant concentration on the upstream slope is negatively correlated with porosity, whereas pollutant concentrations in the downstream slope and recirculation zone are positively correlated with porosity. Under the same conditions, average pollutant concentration in the downstream slope is about 16% lower than the concentration before passing through the spur dike, and the difference between the recirculation zone and downstream slope concentrations is minimal.

(iii) When flow discharge and porosity are identical, pollutant concentrations on both upstream and downstream slopes are negatively correlated with pore size, while concentrations in the recirculation zone are positively correlated with pore size. Overall, pore size has a greater impact on pollutant concentrations on the downstream slope and in the recirculation zone, and a smaller impact on the upstream slope.

(iv) Pollutant concentrations downstream of and within the recirculation zone behind a permeable spur dike are influenced not only by hydraulic conditions but also closely related to structural parameters (porosity and pore size). Variations in flow discharge mainly affect concentration distribution by altering the transport rates and pollutant residence times in water, while porosity and pore size modulate permeability and local flow velocity, thereby influencing the extent to which pollutants enter or remain in specific zones.

Therefore, in the design of ecological spur dike projects for navigation channels, porosity and pore size can be optimized to control downstream pollutant accumulation while maintaining structural stability, thereby balancing hydrodynamic exchange and habitat quality.

Acknowledgments

None.

Funding

This study is supported by the National Key Research and Development Program of China (Grant No.: 2023YFB2604700) and the Chongqing Natural Science Foundation of China (Grant No. CSTB2023NSCQ-LZX0097).

Conflict of interest

Junhui He and Dejian Wei are employees of Pinglu Canal Group Co., Ltd. However, there is no conflict of interest related to the company regarding the results of this study. The authors declared no potential conflicts of interest with respect to the research, authorship, and publication of this article.

Author contributions

Conceptualization: Junhui He, Tao Yu
Formal analysis: Junhui He, Tao Yu
Investigation: Junhui He, Dejian Wei
Methodology: Tao Yu, Dejian Wei, Linfeng Han
Writing–original draft: Junhui He, Tao Yu
Writing–review & editing: Tao Yu, Linfeng Han

Availability of data

The datasets used and analyzed during the current study are available from the corresponding author on reasonable request.

References

1. Giglou AN, McCorquodale JA, Solari L. Numerical study on the effect of the spur dikes on sedimentation pattern. *Ain Shams Eng J*. 2018;9(4):2057-2066.

doi: 10.1016/j.asej.2017.02.007

2. Patel HK, Arora S, Lade AD, Kumar B, Azamathulla HM. Flow behaviour concerning bank stability in the presence of spur dike – A review. *Water Supply*. 2022;23(1):237-258.

doi: 10.2166/ws.2022.418

3. Patel HK, Kumar B. Hydro-morphological behavior around T-shaped spur dikes with downward seepage. *Sci Rep*. 2023;13(1):12345.

doi: 10.1038/s41598-023-37694-w

4. Jafari R, Sui J. Velocity Field and Turbulence Structure around Spur Dikes with Different Angles of Orientation under Ice Covered Flow Conditions. *Water*. 2021;13(13):1844.

doi: 10.3390/w13131844

5. Qi H, Wang J, Zou W, Luo W, Tian W, Li J. Characteristics and mechanism of local scour reduction around spur dike using the collar in clear water. *Sci Rep*. 2024;14(1):12345.

doi: 10.1038/s41598-024-63131-7

6. Ding C, Li C, Song L, Chen S. Numerical Investigation on Flow Characteristics in a Mildly Meandering Channel with a Series of Groynes. *Sustainability*. 2023;15(5):4124.

   doi: 10.3390/su15054124

7. Yang MM, Chen YM. Research on influences and countermeasures of spur dike on ecology of regulation river reach. *J Waterw Harbor*. 2014;35(156):545-549. Available from: https://sdgk.cbpt.cnki.net/portal/journal/portal/client/paper/744654f466b0e59786b115ebc999fd36 [Last accessed on February 10, 2026].

8. Chung S, Choi D, Hwang G, Chung J. Effect of design factors for groynes on diversification of topography and restoration of ecosystems in straight and meandering streams. *Ecol Eng*. 2020;149:105764.

   doi: 10.1016/j.ecoleng.2020.105764

9. Huang T, Lu Y, Liu H. Effects of Spur Dikes on Water Flow Diversity and Fish Aggregation. *Water*. 2019;11(9):1822.

   doi: 10.3390/w11091822

10. Li S, Tong S. Progress and Prospects of Research on Ecological Impact of Channel Regulation Structure. *IOP Conf Ser Earth Environ Sci*. 2021;643(1):012092.

    doi: 10.1088/1755-1315/643/1/012092

11. Montazeri A, Abedini A, Aminzadeh M. Numerical investigation of pollution transport around a single non-submerged spur dike. *J Contam Hydrol*. 2022;248:104018.

    doi: 10.1016/j.jconhyd.2022.104018

12. Wan Y, Huang G, Du H, Yang S, Yang W, Li W. Effects of waterway regulation structures on the planktonic community in the upper Yangtze River. *Ecol Indic*. 2023;155:111049.

    doi: 10.1016/j.ecolind.2023.111049

13. Przyborowski Ł, Cuban Z, Łoboda A, Robakiewicz M, Biegowski S, Kolerski T. The effect of groyne field on trapping macroplastic. Preliminary results from laboratory experiments. *Sci Total Environ*. 2024;921:171184.

    doi: 10.1016/j.scitotenv.2024.171184

14. Zhang X, Dou Z, Chen Z, Zhu W, Wang J, Zhou Z. Uncovering asymmetrical mass transfer in layered porous media: Insights from pore-scale analysis. *J Hydrol*. 2023;623:129790.

    doi: 10.1016/j.jhydrol.2023.129790

15. Divya T, Law AWK, Chong TH, Kuiry SN. Effect of floodplain submergence and riparian vegetation on flow dynamics and mass transport near a spur dike. *Phys Fluids*. 2025;37(7):075123.

    doi: 10.1063/5.0277309

16. Zhang W, Liu B, Zhuo J, Summer W. Numerical simulation on low-water ecological restoration project of straight river channel. *Chin J Hydrodyn*. 2016;31(2):245-252.

    doi: 10.16076/j.cnki.cjhd.2016.02.015

17. Zhao S, Du Y, Wang Y, Yin S, Wang S, Xu J. Wutong River Fish Habitat Survey and Modeling Under Ecological Restoration. *J Hydroecol*. 2019;40(5):1-8.

    doi: 10.15928/j.1674-3075.2019.05.001

18. Wang Y. *Distribution Characteristics of Nutrients around Environmental Restoration Groynes*. Dissertation. Shaanxi University of Science and Technology; 2017.

19. Zhao W, Xie Y, Yu Y, Wang S, Zhang C, Wang J. Study on the influence of different ecological reoxygenation modes on dissolved oxygen in urban rivers. *Environ Ecol*. 2019;1(3):61-66. Available from: http://dianda.cqvip.com/Qikan/Article/Detail?id=7100125748&from=Qikan_Article_Detail [Last accessed on February 10, 2026].

20. Zhang J, Che X, Jia G, Tian C, Chen X. Effects of artificial dams on hydrodynamic characteristics of fish habitats in upper reaches of Yangtze River. *Trans Chin Soc Agric Eng*. 2021;37(5):140-146.

    doi: 10.11975/j.issn.1002-6819.2021.05.016

21. Chen K. Experimental Study on Hydrodynamic Characteristics and Contaminant Concentration Field in Open Channel Intersection [master's thesis]. Xi'an University of Technology; 2019.

22. Yang Z. Study on Pollutant Diffusion of Typical Secondary River Backwater in Three Gorges Reservoir Area [dissertation]. Chongqing Jiaotong University; 2020.

    doi: 10.27671/d.cnki.gcjtc.2020.000659

23. Yang X. Research on the Simulation of Pollutant Dispersion Based on Mike Model——A Case Study of the Middle and Lower Reaches of Hanjiang River [dissertation]. Wuhan University; 2018.

24. Iqbal S, Pasha GA, Ghani U, Ullah MK, Ahmed A. Flow Dynamics Around Permeable Spur Dike in a Rectangular Channel. *Arab J Sci Eng*. 2021;46(5):4999-5011.

    doi: 10.1007/s13369-020-05205-y

25. Han X, Lin P, Parker G. Numerical modelling of local scour around a spur dike with porous media method. *J Hydraul Res*. 2022;60(6):970-995.

    doi: 10.1080/00221686.2022.2106589

26. Qin J, Zhong D, Wu T, Wu L. Sediment exchange between groin fields and main-stream. *Adv Water Resour*. 2017;108:44-54.

    doi: 10.1016/j.advwatres.2017.07.015

27. Haider R, Qiao D, Yan J, Ning D, Pasha GA, Iqbal S. Flow Characteristics Around Permeable Spur Dike with Different Staggered Pores at Varying Angles. *Arab J Sci Eng*.

2022;47(4):5219-5236.

doi: 10.1007/s13369-021-06435-4

28. Li H, Lv J, He X, Bao Y, Nsabimana G. Precipitation-dependent sensitivity of suspended sediment concentration to turbidity in a mountainous river in southwestern China. *Ecol Indic*. 2024;159:111644.

doi: 10.1016/j.ecolind.2024.111644

29. Ministry of Water Resources of the People's Republic of China. *Code for discharge measurement in rivers (GB 50179-2015)*. China Planning Press; 2016.

30. Dimitriadis P, Koutsoyiannis D, Iliopoulou T, Papanicolaou P. A Global-Scale Investigation of Stochastic Similarities in Marginal Distribution and Dependence Structure of Key Hydrological-Cycle Processes. *Hydrology*. 2021;8(2):59.

doi: 10.3390/hydrology8020059

31. Xu B. *Experimental Study on Water Flow Characteristics of Permeable Butyl Dam under Different Voids*. Master's Thesis. Chongqing Jiaotong University; 2019.

doi: 10.27671/d.cnki.gcjtc.2019.001011